

Elastic shear buckling of cold-formed steel channels with edge stiffened web holes

Author

Gatheeshgar, Perampalam, Poologanathan, Keerthan, Gunalan, Shanmuganathan, Dimopoulos, Christoforos, Vasdravellis, George

Published

2023

Journal Title

Thin-Walled Structures

Version

Accepted Manuscript (AM)

DOI

[10.1016/j.tws.2023.110551](https://doi.org/10.1016/j.tws.2023.110551)

Rights statement

© <year>. This manuscript version is made available under the CC-BY-NC-ND 4.0 license
<https://creativecommons.org/licenses/by-nc-nd/4.0/>

Downloaded from

<http://hdl.handle.net/10072/428527>

Griffith Research Online

<https://research-repository.griffith.edu.au>

Elastic shear buckling of cold-formed steel channels with edge stiffened web holes

Perampalam Gatheeshgar^{a,*}, Keerthan Poologanathan^b, Shanmuganathan Gunalan^c,
Christoforos Dimopoulos^a, George Vasdravellis^d

^{a,*}School of Computing, Engineering & Digital Technologies, Teesside University, Middlesbrough, UK

^b Faculty of Engineering and Environment, Northumbria University, Newcastle upon Tyne, UK

^cSchool of Engineering and Built Environment, Griffith University, Queensland, Australia

^dInstitute for Infrastructure and Environment, Heriot-Watt University, Edinburgh, UK

Abstract

Cold-formed steel (CFS) beams are commonly deployed in construction with web holes to accommodate service conduits. The web holes are subjected to stiffening methods aiming to restore the load-carrying strength reduction. In the shear design of CFS channels with stiffened web holes, the elastic shear buckling strength is the basis for the design irrespective of the available post-buckling strength. Therefore, this paper investigates the elastic shear buckling characteristics of CFS channels with stiffened circular web holes, which is still unresearched. Numerical simulations were conducted using the Abaqus finite element analysis software to study the elastic shear buckling response. Parametric studies were then performed, where a data pool was generated for CFS channels with no web holes, unstiffened web holes, and stiffened web holes, covering a range of parameters including web slenderness, web hole size, corner radius and edge stiffening element length. It was shown that edge stiffening of the web hole improves the shear buckling capacity compared to the CFS channels with no web holes and unstiffened web holes. New unified design proposals to estimate the elastic shear buckling strength of CFS channels with no web holes, unstiffened web holes, and edge stiffened web

25 holes were developed based on the generated data. The new unified design proposals of
26 modified shear buckling coefficient and equivalent thickness method offer accurate elastic
27 shear buckling strength predictions.

28

29 **Keywords:** Cold-formed steel channels; Stiffened web holes; Shear buckling; Elastic shear
30 buckling analyses; New design equations.

31

32 **1. Introduction**

33 In steel buildings, web holes are provided in cold-formed steel (CFS) channels to
34 accommodate service conduits. Hence the overall depth of a floor system can be maintained
35 relatively low. These web holes reduce the load-carrying capacity of a CFS beam under various
36 loading conditions, including bending, shear, web crippling, and combined actions. Introducing
37 stiffeners in the vicinity of the web holes improves the load-carrying capacity of CFS channels.
38 Fig. 1 shows a CFS channel with a stiffened web hole. The stiffeners in the vicinity of the web
39 holes alleviate the buckling instabilities of the weakened web due to the web holes. In this
40 context, understanding the elastic buckling characteristics, including the shear buckling
41 characteristics of CFS channels with unstiffened and stiffened web holes is important for
42 encouraging wider use in construction.

43



44

45 Fig 1: Cold-formed steel channel with a stiffened web hole.

46 The shear behaviour of CFS beams has been investigated extensively by Keerthan and
47 Mahendran [1-6] for lipped channels and hollow flange channels, Pham and Hancock [7, 8] for
48 lipped channels and SupaCee Channels, Gatheeshgar et al. [9, 10] for optimised CFS beams.
49 The abovementioned studies compared the results with international design codes (Eurocode
50 [11], North American [12], and Australian and New Zealand [13]) and proposed modifications
51 to the design provisions which included the development of the direct strength method (DSM)
52 design for CFS channels subject to shear.

53 Further, several studies [14-30] into the shear behaviour of CFS channels with un-
54 stiffened web holes have been carried out, identifying the influence of web hole size, shape,
55 and location on the degree of shear capacity reduction. Most of these focused their attention on
56 circular openings [20, 22-25, 27, 29, 30], however, there were different studies which
57 investigated the effect of non-circular openings, for example, square, rectangular, elliptical,
58 slotted and other elongated holes [14-21, 28]. Experimental and/or numerical methods were
59 employed in these studies. Alternative DSM-based design equations were proposed for the
60 shear strength of CFS channels. Keerthan and Mahendran [31, 32] studied various stiffening
61 techniques aiming to restore the original shear capacity of hollow flange beams. Recently, Chen
62 et al. [33] and Kanthasamy et al. [34] investigated shear behaviour of CFS lipped channels and
63 hollow flange channels, respectively, with edge stiffened web holes. Their results showed that
64 edge stiffeners were capable to increase the ultimate shear capacity compared to that of
65 unstiffened web holes. Several reduction factor formulae have been developed to account for
66 the un-stiffened and stiffened web holes. Overall, the abovementioned studies discovered the
67 presence of post-buckling strength and tension field action on the ultimate shear strength of the
68 CFS channels with and without web holes.

69 Despite the post-buckling strength and tension field action under the shear load in the
70 CFS channel, elastic buckling strength is a fundamental parameter in the design of CFS

71 members. The assessment of elastic shear buckling strength enables us to determine the degree
72 of post-buckling strength exhibited by a CFS channel. A considerable body of research has
73 been undertaken on elastic shear buckling behaviour of CFS channels, such as by Keerthan and
74 Mahendran [2, 35, 36] and Pham and Hancock [37, 38]. Keerthan and Mahendran [2, 35, 36]
75 explored the fixity level at the web-flange juncture of CFS lipped channels and various hollow
76 flange sections, and proposed shear buckling coefficients that should be considered for accurate
77 shear capacity prediction. Pham and Hancock [37, 38] utilised the spline finite strip method to
78 investigate the effect of flange width on the shear buckling coefficient of CFS lipped and
79 unlipped channels. Subsequently, shear buckling response of CFS lipped channels with central
80 circular and square holes, was numerically studied by Pham [39], with new predictive formulae
81 proposed to estimate the reduced shear buckling coefficient. However, the elastic shear
82 buckling behaviour of CFS channels with edge stiffened web holes and simple procedures to
83 estimate the elastic shear buckling strength are yet to be explored.

84 Complementing the existing research, this study intends to investigate the shear
85 buckling characteristics of the CFS channels with stiffened web holes. CFS channels with no
86 web holes and un-stiffened web holes were also considered as reference sections and for
87 comparison purposes. Finite element (FE) analysis using Abaqus [40] software was performed
88 to closely examine the shear buckling behaviour as numerical methods are the convenient
89 practical option available to determine the elastic buckling strength. Unified design equations
90 are proposed to estimate the elastic shear buckling strength of CFS channels with no holes,
91 unstiffened web holes, and stiffened web holes considering the effect of geometric and
92 mechanical parameters.

93 2. Elastic shear buckling

94 2.1. Elastic shear buckling of isolated plates

95 The buckling response of flat plates has been understood well based on numerous
96 research studies from early days. These studies have led to the development of elastic buckling
97 solutions for rectangular plates subject to a range of practical load cases. According to
98 Timoshenko and Gere [41], the shear elastic buckling stress (τ_{cr}) of a rectangular plate is
99 estimated by Eq. 1.

$$\tau_{cr} = \frac{k_v \pi^2 E}{12(1 - \nu^2)} \left(\frac{t}{d_1} \right)^2 \quad (1)$$

100 Here, E and ν are the Young's modulus and Poisson's ratio, respectively. The dimensions of
101 the rectangular plate, thickness (t) and clear height (d_1), are the other parameters. k_v is the
102 shear buckling coefficient of the plate. The value of the coefficient is decided based on the
103 aspect ratio of the plate and boundary conditions (simply supported, fixed or free) at the edges.
104 For a simply supported square plate the buckling coefficient is 9.34. This value will gradually
105 reduce to 5.34 for a very lengthy plate.

106 The elastic shear buckling strength (V_{cr}) can be related to the elastic shear buckling
107 stress by $V_{cr} = A_w \tau_{cr}$, where $A_w = d_1 t$. By use of this, the elastic shear buckling capacity
108 (V_{cr}) can be estimated as follows in Eq. 2.

$$V_{cr} = \frac{k_v \pi^2 E t^3}{12(1 - \nu^2) d_1} \quad (2)$$

109

110 2.2. Elastic shear buckling of channels

111 The elastic shear buckling strength of a CFS channel is estimated through Eq. 2 as the
112 web portion is subjected to buckling under the shear load. Appropriate boundary conditions
113 should be considered at the web-flange juncture. This boundary condition could be simply
114 supported, fixed, and in between simply supported and fixed. The conventional method of

115 design is assuming the web portion is simply supported at the web-flange juncture, which leads
 116 to a conservative design. Following Lee et al. [42]'s study, Keerthan and Mahendran [2, 35,
 117 36] explored that for CFS channels web-flange fixity level is in between simply supported and
 118 fixed (clamped) support and the degree of fixity level may vary according to CFS channel
 119 cross-sections.

120 The following simple equations (Eq. 3 – Eq. 5) were proposed by Keerthan and
 121 Mahendran [2, 35, 36] to determine the shear buckling coefficients (k_v) of CFS channels. The
 122 shear buckling coefficient depends on the boundary conditions along the edges and the aspect
 123 ratio of the channel. Hence, the shear buckling coefficient (k_v) has been formed as a function
 124 of shear buckling coefficient of the web panel with simple-simple (k_{ss}) and simple-fixed (k_{sf})
 125 boundary conditions. While k_{ss} and k_{sf} are sensitive to the aspect ratio (a/d_1 , a = shear span
 126 and d_1 = clear height of the web).

127

$$k_v = k_{ss} + k_n(k_{sf} - k_{ss}) \quad (3)$$

128

$$k_{ss} = 4 + \frac{5.34}{(a/d_1)^2} \quad \text{for } \frac{a}{d_1} < 1 \quad (4.1)$$

$$k_{ss} = 5.34 + \frac{4}{(a/d_1)^2} \quad \text{for } \frac{a}{d_1} \geq 1 \quad (4.2)$$

129

$$k_{sf} = \frac{5.34}{(a/d_1)^2} + \frac{2.31}{(a/d_1)} - 3.44 + 8.39(a/d_1) \quad \text{for } \frac{a}{d_1} < 1 \quad (5.1)$$

$$k_{sf} = 8.98 + \frac{5.61}{(a/d_1)^2} - \frac{1.99}{(a/d_1)^3} \quad \text{for } \frac{a}{d_1} \geq 1 \quad (5.2)$$

130

131 Degree of fixity level at the web-flange juncture is represented by the coefficient k_n .
 132 Based on the analyses Keerthan and Mahendran [36] discovered that the fixity level at the web-
 133 flange juncture of lipped channel is 23%, which means $k_n = 0.23$. For other types of cross-

134 sections including hollow flange sections, different k_n values have been proposed [2]. Hence,
 135 based on the abovementioned equations shear buckling strength of CFS sections can be
 136 estimated.

137

138 **2.3. Elastic shear buckling of channels with web holes**

139 Pham [39] developed equations to estimate the elastic shear buckling capacity of CFS lipped
 140 channels with centred circular and square web holes. The study indicated that the shear
 141 buckling coefficients reduce as the hole sizes increases. The reduction in the shear buckling
 142 coefficient is dramatic and nonlinear when the hole sizes are large, while the shear buckling
 143 coefficient reduces slightly when the hole sizes are small. Pham [39] proposed reduction factors
 144 for different ranges of web hole (d_w)-to- web depth (D) ratios. The proposed reduction factors
 145 can be directly applied to the shear buckling coefficients of channels without web holes in order
 146 to determine the shear buckling coefficients of channels with unstiffened web holes. The
 147 proposed equations for the CFS channels with centred circular web holes are demonstrated in
 148 Eq. 6.

$$k_{v,UH} = k_{v,NH} \left[1 - 0.5 \left(\frac{d_w}{D} \right) - 4.2 \left(\frac{d_w}{D} \right)^2 \right] \quad \text{for } \frac{d_w}{D} \leq 0.2 \quad (6.1)$$

$$k_{v,UH} = k_{v,NH} \left[1.15 - 2.35 \left(\frac{d_w}{D} \right) + 1.5 \left(\frac{d_w}{D} \right)^2 \right] \quad \text{for } 0.2 < \frac{d_w}{D} < 0.6 \quad (6.2)$$

$$k_{v,UH} = k_{v,NH} \left[0.6 - 0.53 \left(\frac{d_w}{D} \right) \right] \quad \text{for } \frac{d_w}{D} \geq 0.6 \quad (6.3)$$

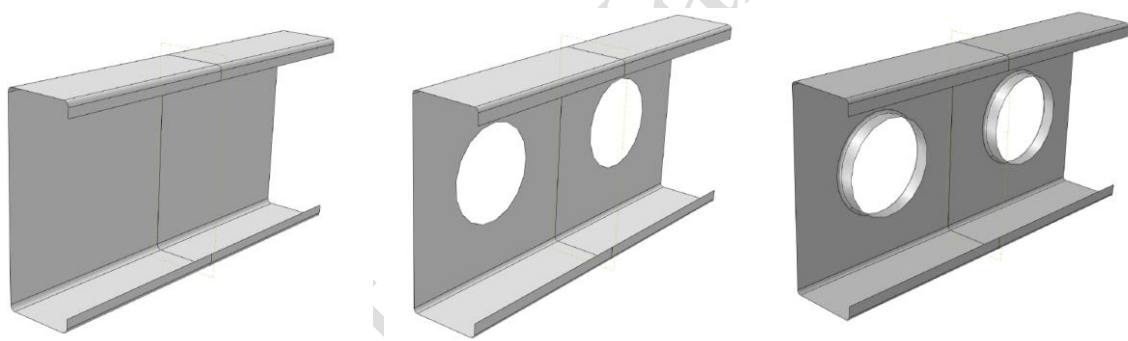
149

150 Here, $k_{v,UH}$ is the shear buckling coefficients of channels with unstiffened web holes and
 151 $k_{v,NH}$ ($= k_v$) is the shear buckling coefficients of channels with no web holes. Hence, based
 152 on the abovementioned equations shear buckling capacity of CFS sections with unstiffened
 153 circular web holes can be estimated.

154 **3. Numerical modelling and data generation**

155 **3.1. General modelling assumptions**

156 The elastic shear buckling strengths of the CFS channels with no web holes, unstiffened
157 web holes, and stiffened web holes were investigated by means of the FE simulation software,
158 Abaqus [40]. Ideal FE models were developed with a three-point loading arrangement while
159 maintaining aspect ratios of 1.0. The aspect ratio of 1.0 minimises the possibilities of bending
160 failure and allows the sections to predominantly buckle under shear. The circular web holes
161 without and with stiffeners were created at the centre of shear spans. Fig. 2 shows the generated
162 CFS channels with no web holes, unstiffened web holes, and stiffened web holes. The Young's
163 modulus (E) and the Poisson's ratio (ν) were considered as 200 GPa and 0.3, respectively for
164 CFS material.



165 (a) Channels with no holes (b) Channels with unstiffened webholes (c) Channels with stiffened web holes

166 Fig. 2: Developed FE models for the analysis

167
168 The basic S4R shell element available in the Abaqus element library was employed to
169 define the element type. The S4R shell element has inherent characteristics of reduced
170 integration, allows large strain deformations, and converges to shear flexible and classical
171 theories when the shell thickness is thick and thin, respectively. A uniform mesh density of 5
172 mm \times 5 mm was used for the flat regions while the corners of the cross-section and stiffener
173 location were refined with 1 mm \times 5 mm mesh dimensions as shown in Fig. 3.

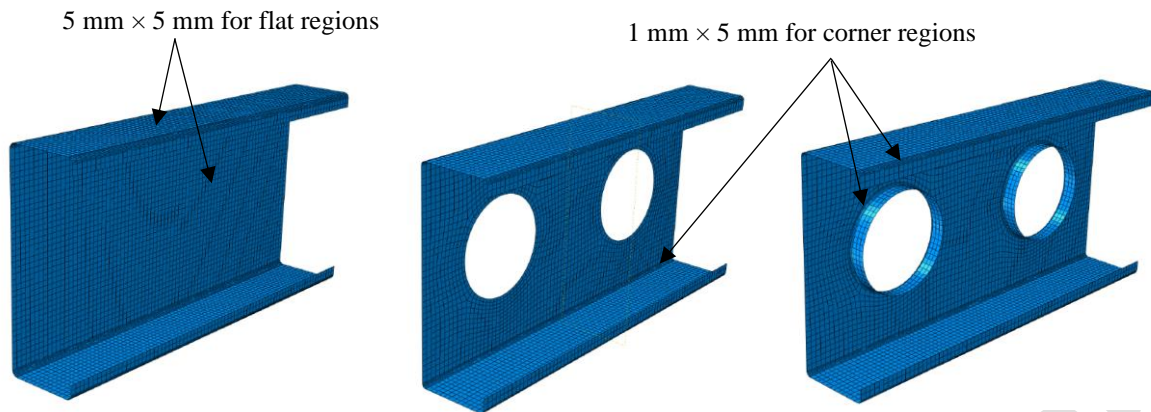


Fig. 3: Meshing scheme used in FE models

174

175

176

177

178

179

180

181

182

183

184

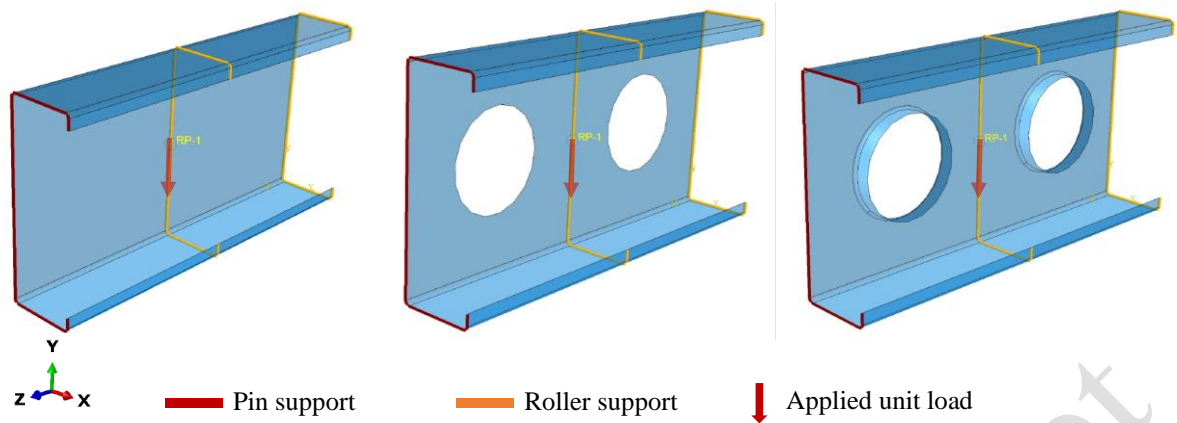
185

186

187

188

Simply supported boundary conditions were applied to the developed FE model at three locations of two edges and mid-span. The assigned simply supported boundary conditions are depicted in Fig. 4. Here, the translations in x- and y-directions were restrained at both ends, adding that the translation in the z-direction was restrained at one end to simulate the pin support leaving the other end to act as roller support. At the mid-span, translation in the x- and z-directions were restrained. Rotation about the z-axis was fixed at end supports and loading plane to avoid the torsional effect in shear buckling. It is worth noting that in order to ensure the shear flow of the full cross-section, all these boundary conditions were applied to the entire cross-section elements of web, flanges and lips. A unit load was then applied through the web at the mid-span to allow the cross-section to buckle under shear (see Fig. 4). Similar element type, meshing scheme, and boundary conditions were also reported in past studies [35, 36, 43] to explore the elastic shear buckling response of cold-formed sections.



189

190

191

Fig. 4: Assigned boundary conditions to FE models

192

193

194

195

196 3.2. Data generation

197

198

199

200

201

202

203

204

205

206

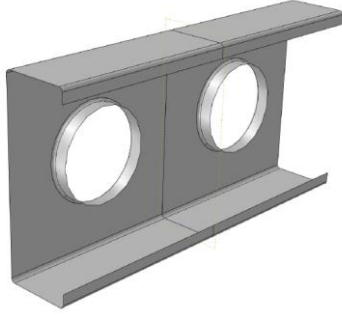
207

208

The developed FE models were then subjected to eigenvalue buckling analysis to generate the shear buckling modes. The lowest buckling mode and eigenvalue were assumed as critical shear buckling mode and shear buckling force, respectively.

For the data generation, a series of numerical analyses were carried out using three-dimensional modelling characteristics explained in Section 3.1. The numerical analyses were conducted on several combinations that can affect the shear buckling. In total, 551 numerical results were generated. This included 29 different lipped channels available commercially, 87 lipped channels with unstiffened circular web holes, and 435 lipped channels with stiffened circular web holes. The range of cross-sectional dimensions and other parameters considered for the data generation is presented in Table 1. Three different web hole ratios of 0.3, 0.5, and 0.8 and five different stiffener lengths 5, 10, 15, 20, and 25 mm were considered to take the effect of web hole and stiffener response on shear buckling. Here, the web hole ratio is defined as the ratio between the diameter of the web hole and the clear height of the web. The corner radius that forms at the connecting location of the web and stiffener was taken as 2 mm.

Table 1: Range of cross-section dimensions and other parameters considered in data generation

Lipped Channel	Variables	Range
	Web height	100 mm -300 mm
	Flange width	50 mm – 70 mm
	Lip depth	10 mm – 15 mm
	Thickness	1.2 mm – 3 mm
	Web hole ratio	0.3 – 0.8
	Stiffener length	5 mm – 25 mm

210

211 4. Analysis and discussion of results

212 4.1. Channels with no web holes

213 The results of CFS lipped channels with no web holes were compared against the
 214 Keerthan and Mahendran [36]’s elastic shear buckling capacity estimation (Eq. 2 - Eq. 5). The
 215 comparison is illustrated in Fig. 5 in terms of elastic shear buckling strength predicted and
 216 back-calculated shear buckling coefficient. Keerthan and Mahendran [36] proposed to impose
 217 a 23% fixity level at the web-flange juncture which leads to a shear buckling coefficient k_v
 218 =10.09 for lipped channels with flange width (b)- to-clear web height (d_1) ratio greater than
 219 0.3. For smaller ratios k_v =9.34 can be used. From Fig 5(a), it is observed that there is a good
 220 agreement between the elastic shear buckling capacities obtained from FE analyses ($V_{cr,FE}$)
 221 and predictions from Keerthan and Mahendran [36] ($V_{cr,KM}$), with a mean $V_{cr,KM} / V_{cr,FE}$ ratio
 222 of 0.99 and a coefficient of variation (COV) of 0.031. The described comparison also
 223 demonstrates the ability of the developed FE models in predicting the elastic shear buckling
 224 strength and the possibility of extending FE models with similar modelling characteristics.

225

226
227
228
229
230
231
232
233
234
235
236
237
238
239
240
241
242
243
244
245
246
247
248
249
250

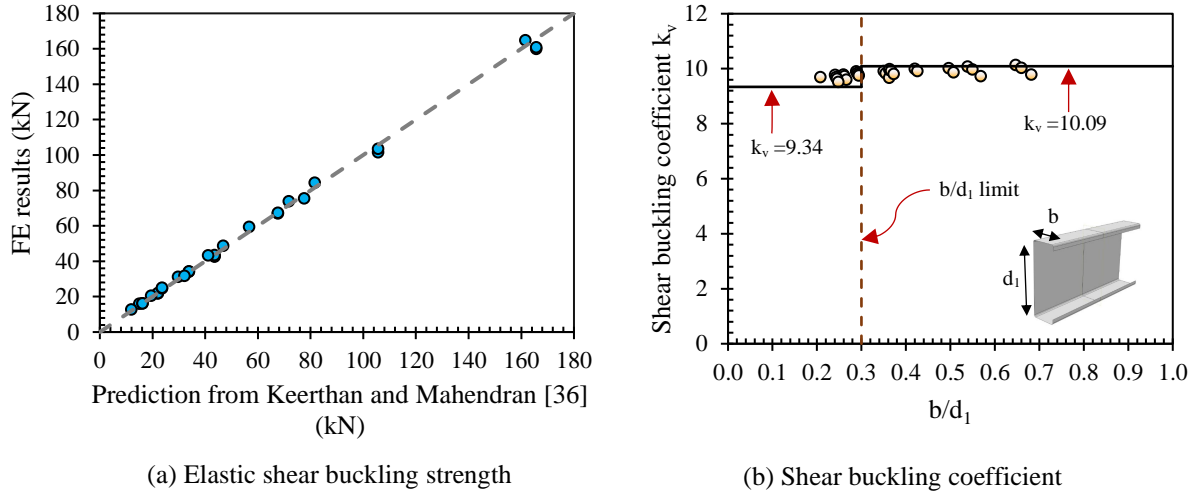
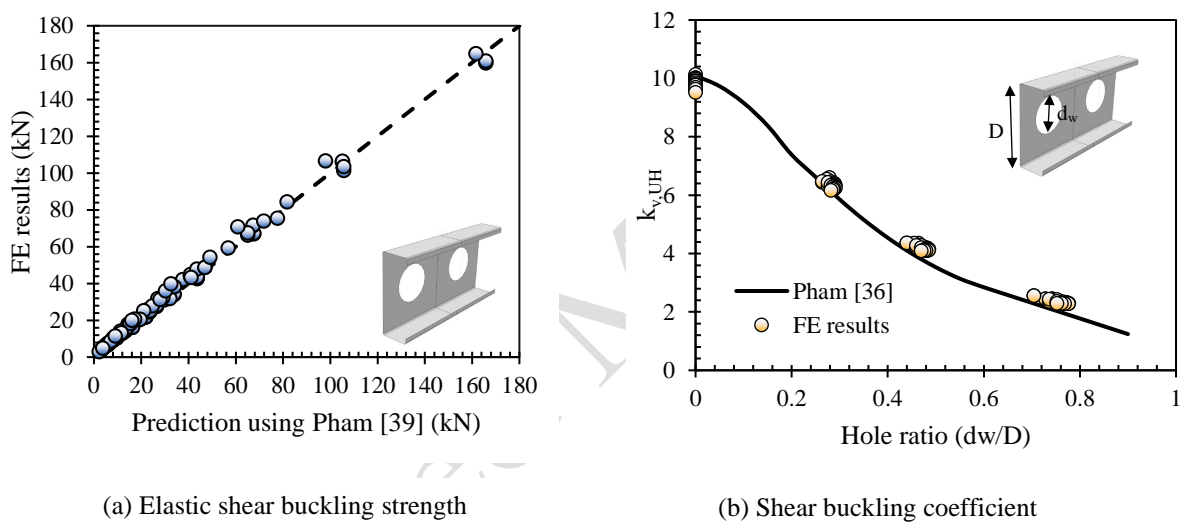


Fig. 5: Comparison of the FE results against Keerthan and Mahendran [36]'s prediction for lipped channels with no web holes.

4.2. Channels with unstiffened web holes

The FE elastic shear buckling capacity data generated for CFS lipped channels with unstiffened circular web holes were compared against the design proposal (Eq. 2 and Eq. 6) by Pham [39]. It should be noted that the hole ratio considered by Pham [39] is based on the full depth of the web (D) which is slightly different from the current study where hole ratio is based on clear height of the web (d_1). Therefore, for a reliable comparison, the considered hole ratios in the current study (0.3, 0.5, and 0.8) were converted to web hole diameter (d_w)-to-full web height (D) ratios. Fig. 6 depicts the comparison of the FE results against the prediction from Pham [39]. According to Pham [39], the shear buckling coefficient for CFS lipped channels with unstiffened web holes ($k_{v,UH}$) is calculated applying a reduction factor for the shear buckling coefficient for CFS lipped channels with no web holes ($k_{v,NH}$). Hence, $k_{v,NH} = 10.09$ was used to calculate the $k_{v,UH}$ and then elastic shear buckling strength was estimated. A reasonable agreement can be observed (see Fig. 6(a)) in terms of elastic shear buckling capacity from FE analyses ($V_{cr,FE}$) and prediction from Pham [39] ($V_{cr,P}$), with a mean $V_{cr,P} / V_{cr,FE}$ ratio of 0.91 and a COV of 0.071.

251 Further, back-calculated shear buckling coefficient from FE results for CFS channels
 252 with unstiffened web holes ($k_{v,UH}$) are plotted against Pham [39]'s elastic shear buckling
 253 coefficient proposal, shown in Fig. 6(b). Pham [39]'s shear buckling coefficient proposal
 254 demonstrated a small level of conservatism with back-calculated shear buckling coefficient
 255 from FE results for CFS channels with unstiffened web holes. These comparisons and close
 256 agreements also indicate that the established FE models are reliable to simulate the elastic shear
 257 buckling response with unstiffened web holes and similar modelling characteristics can be used
 258 for stiffened web hole cases.

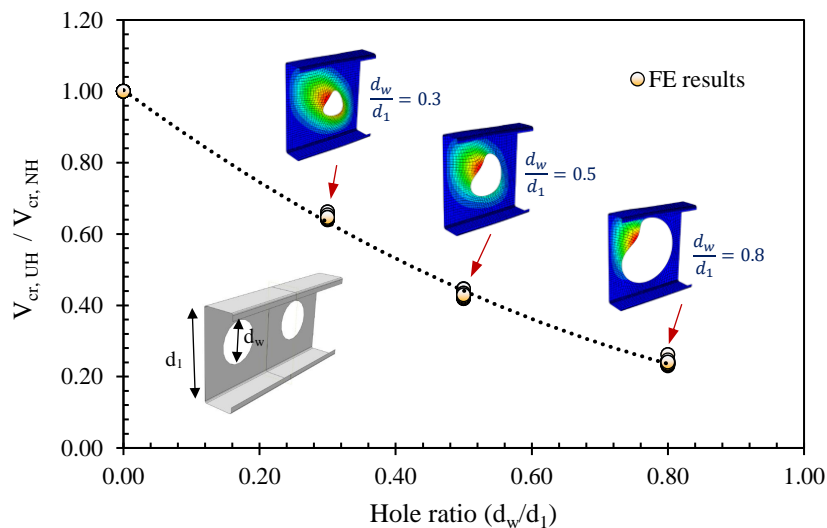


259 (a) Elastic shear buckling strength
 260 (b) Shear buckling coefficient
 261 Fig. 6: Comparison of the FE results against Pham [39] prediction for lipped channels with unstiffened circular
 262 web holes.

263 Elastic shear buckling strength reduction observed for the considered 0.3, 0.5, and 0.8
 264 web hole ratios is plotted in Fig. 7. A notable reduction in elastic shear buckling capacity was
 265 noticed for each web hole ratio. The reduction in elastic shear buckling capacity was defined
 266 as the ratio between elastic shear buckling capacity of CFS channels with unstiffened web holes
 267 ($V_{cr,UH}$) and no holes ($V_{cr,NH}$). It can be observed that irrespectively of the range of different
 268 parameters (web heights and thicknesses) the degree of elastic shear buckling strength
 reduction merges to closer values for particular web hole ratios. The average degree of elastic

269 shear buckling capacity reductions were 65%, 42%, and 24% for 0.3, 0.5, and 0.8 web hole
270 ratios, respectively.

271 The typical elastic shear buckling shapes obtained from FE analyses for web hole ratios
272 are depicted in Fig. 7. It can be observed that shear buckling is not symmetric and is more
273 severe at the top corner compared to the bottom corner. It is worth noting that ideal FE models
274 were developed with a three-point loading arrangement, which induces some degree of bending
275 stress. As a result, the developed compressive stress in the top flange and lip influences shear
276 buckling at the top corner. A similar observation has also been reported elsewhere [39].



277
278 Fig. 7: Elastic shear buckling capacity reduction and typical buckling mode shapes associated with web hole
279 ratios

281 4.3. Channels with stiffened web holes

282 FE results of the CFS channels with stiffened web holes are discussed herein. Elastic
283 shear buckling modes obtained from FE analyses were compared with the elastic shear
284 buckling modes of corresponding CFS channels with unstiffened web holes and no holes. Fig.
285 8 shows the buckling mode shapes of 250×70×15×2.0 CFS channels under different cases.
286 These buckling modes reflect the elastic shear buckling modes shapes. More severe shear

287 buckling at the top corner of the CFS channels for unstiffened web holes and stiffened web
288 holes were noticed. This is due to induced bending moment and resulting compressive forces
289 at flange and lip which influences the weakened web, as explained in Section 4.2. Further, it
290 can be noticed that a severe shear buckle happens at the edge of the web hole as depicted in
291 Fig. 8(b) when the holes are unstiffened. However, the inclusion of stiffeners around the edge
292 of holes strengthens the edge and as a result, the severe shear buckle approaches the top corner
293 solid region.

294 From the FE analyses, the buckling mode shape with increasing stiffener length was
295 closely observed. Fig. 9 illustrates the shear buckling mode shape of the $250 \times 70 \times 15 \times 2.0$ CFS
296 channel with a 0.5 web hole ratio and different stiffener lengths. When the stiffener length is 5
297 mm, there is no buckling in the stiffener and shear buckling occurs as a whole. However, for
298 the increasing stiffener length, the stiffener displays instability and buckles individually, as
299 depicted in Fig. 9 (c-e). This is because the higher slenderness of the stiffener when the stiffener
300 length increases. Despite the individual buckling of the stiffener with increased length, elastic
301 shear buckling capacity improves with stiffener length, however, the degree of improvement is
302 reducing.

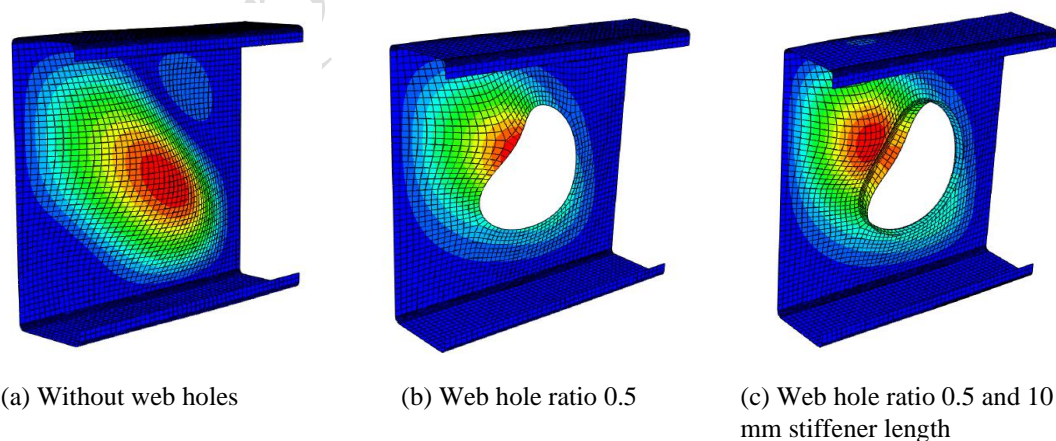


Fig. 8: Elastic buckling mode shapes of $250 \times 70 \times 15 \times 2.0$ CFS channel

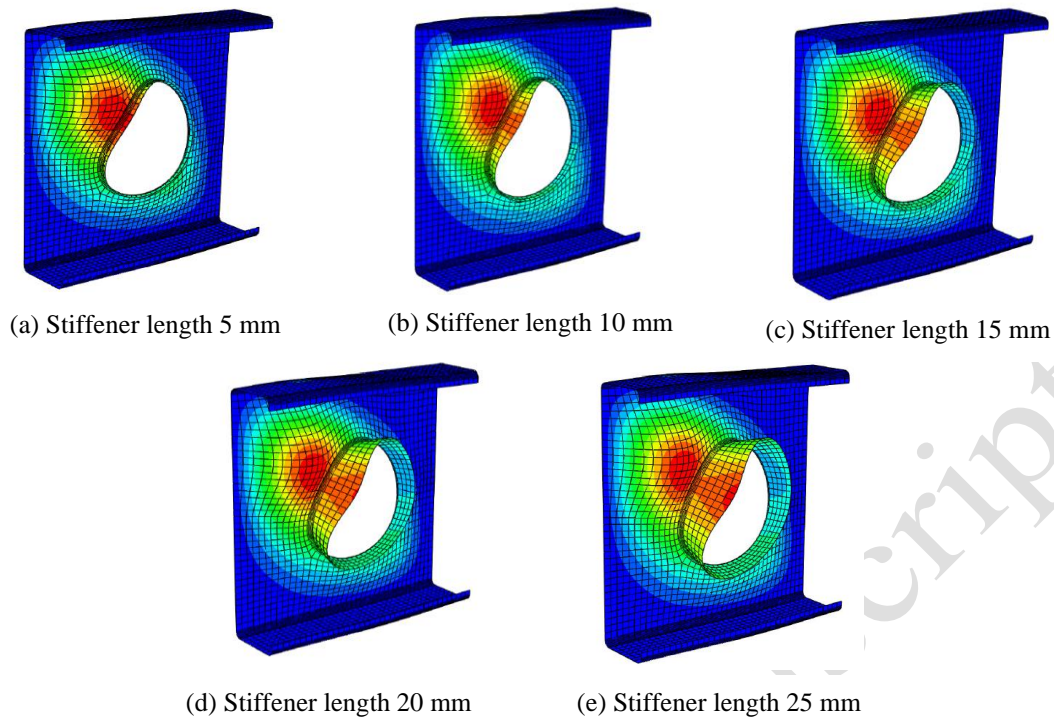
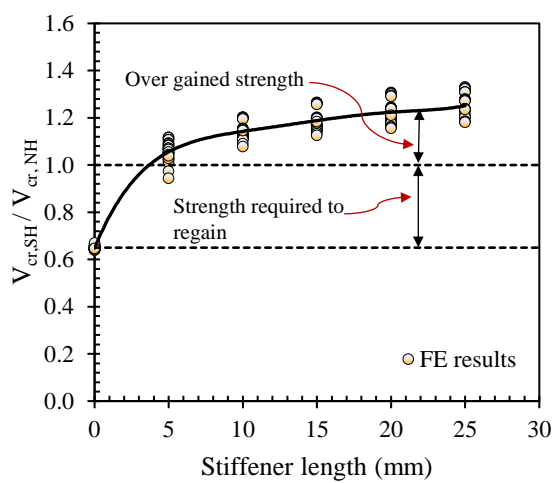
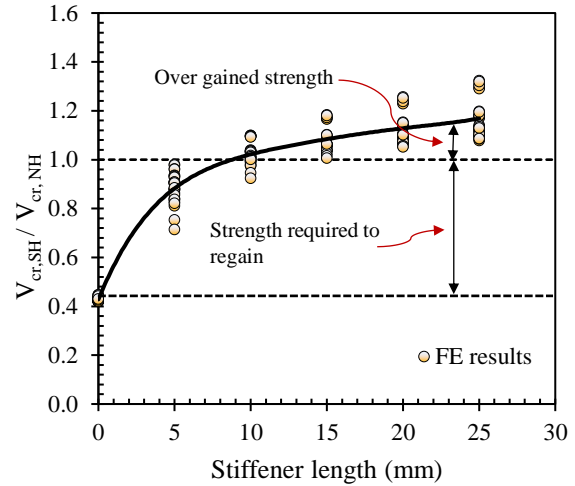


Fig. 9: Elastic buckling mode shapes of 200×50×10×2.0 CFS channel with 0.5 web hole ratio and different stiffener lengths

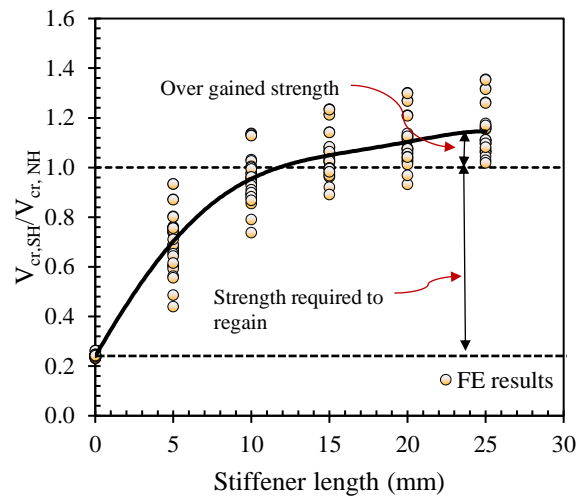
The trend for the degree of shear buckling capacity improvement can be observed in Fig. 10, where elastic shear buckling strength improvement - the ratio between elastic shear buckling capacity of CFS channels with stiffened web holes ($V_{cr,SH}$) and with no holes ($V_{cr,NH}$) - is plotted against the stiffener length. The edge stiffener plays a positive role for the improvement of the elastic shear buckling capacity and the degree of improvement is reduced with stiffener length. Further, it was noticed that the reduced elastic shear buckling strength due to the web holes can be regained effectively with edge stiffener ($V_{cr,SH} = V_{cr,NH}$). It is worth noting that the use of higher stiffener length has led to gaining strength beyond the elastic shear buckling strength of CFS channels with no holes ($V_{cr,SH} > V_{cr,NH}$). Therefore web holes can be edge stiffened and effectively used to enhance the elastic shear buckling strength.



(a) Hole ratio 0.3



(b) Hole ratio 0.5



(c) Hole ratio 0.8

319

320 Fig. 10: Elastic shear buckling strengths of CFS channels with stiffened web holes reference to no holes for
 321 different stiffener lengths

322 5. Design proposals for elastic shear buckling strength

323 It has been identified that there are no design equations available in the literature to
 324 estimate the elastic shear buckling strength of CFS channels with stiffened web holes.

325 Therefore, new design equations are proposed in the subsequent sections, reflecting the
 326 observations made in Section 4.

327 **5.1. Modified shear buckling coefficient**

328 For CFS channels with unstiffened web holes, Pham [39] proposed that elastic shear
329 buckling strength can be estimated through a modified shear buckling coefficient. The shear
330 buckling coefficient of CFS channels with unstiffened holes ($k_{v,UH}$) was developed as a
331 function of web hole ratio, however, separate equations were proposed for different web hole
332 ratio regions (Eq. 6). A unified shear buckling coefficient (k_v) to cover the full range was
333 developed in the current study. The unified shear buckling coefficient (k_v) can be applicable
334 for CFS channels with no holes, unstiffened web holes, and stiffened web holes. The unified
335 shear buckling coefficient (K_v) was formed as a function of web hole ratio, the slenderness of
336 the stiffener, corner radius (at the location where stiffener connected with web)-to-thickness
337 ratio, and stiffener length-to-clear height of the web ratio.

338 It is proposed that the elastic shear buckling strength of a CFS lipped channels can be
339 determined by

$$V_{cr} = \frac{k_v \pi^2 E t^3}{12(1 - \nu^2) d_1} \quad (7)$$

340 where k_v is the unified shear buckling coefficient. This may be approximated as follows:

341

- 342 • For CFS channels with no web holes:

$$k_v = k_{v,NH} \quad (8)$$

343 $k_{v,NH}$ can be estimated using Keerthan and Mahendran [36]'s proposal (Eq. 3 - Eq.5) taking
344 23% fixity level for lipped channels.

345

- 346 • For CFS channels with unstiffened web holes:

$$k_v = k_{v,UH} \quad (9.1)$$

347 Here,

$$k_{v,UH} = k_{v,NH}\lambda_1 \quad (9.2)$$

348 $k_{v,NH}$ can be estimated using Eq. 8 while λ_1 is the factor to take into account the influence of
 349 unstiffened web holes. λ_1 may be estimated by:

$$\lambda_1 = \left[1 - 1.14 \left(\frac{d_w}{d_1} \right) - 0.24 \left(\frac{d_w}{d_1} \right)^2 + 0.24 \left(\frac{d_w}{d_1} \right)^3 + 0.46 \left(\frac{d_w}{d_1} \right)^4 \right] \quad (9.3)$$

350 where $\left(\frac{d_w}{d_1} \right)$ is the ratio between the diameter of the unstiffened web hole (d_w) and clear height
 351 of the web (d_1).

352

353 • For CFS channels with stiffened web holes:

$$k_v = k_{v,SH} \quad (10.1)$$

354 Here,

$$k_{v,SH} = k_{v,NH}\lambda_1\lambda_2 = k_{v,UH}\lambda_2 \quad (10.2)$$

355 $k_{v,NH}$ and λ_1 can be estimated using Eq. 8 and Eq. 9, respectively, as explained above. Here,
 356 λ_2 takes the influence of the stiffener and related parameters: web hole ratio $\left(\frac{d_w}{d_1} \right)$ and
 357 normalised factor (ϕ) associated with the stiffener parameters. The physical meaning
 358 underlying this normalised factor is to capture the effect of edge stiffener parameters, which
 359 include the ratio between stiffener length-to-thickness, stiffener length-to-clear height of the
 360 web, and corner radius where the stiffener is connected to the web-to-thickness. From the
 361 analysis, it was noticed that these parameters influence the elastic shear buckling strength of
 362 CFS channels with stiffened web holes. λ_2 may be determined by:

$$\lambda_2 = \left[0.50 + 4.37 \left(\frac{d_w}{d_1} \right) \phi^{0.23} \right] \quad (10.3)$$

363 where normalised factor (ϕ) may be approximated by

$$\phi = \sqrt{\left(\frac{s}{t}\right) \left(\frac{s}{d_1}\right) \left(\frac{r_s}{t}\right)} \quad (10.4)$$

364

365 Here, s is the stiffener length while r_s is the corner radius at the location where stiffener is
 366 connected with the web.

367

368 **5.2. Equivalent thickness method**

369 An equivalent thickness method to consider the influence of the unstiffened and
 370 stiffened web holes is proposed in this section. The proposed equivalent thickness method
 371 considered the influence of the web hole ratio $\left(\frac{d_w}{d_1}\right)$ and the normalised factor (ϕ) to represent
 372 the stiffener parameters, as explained in Section 5.1. Hence, the elastic shear buckling strength
 373 of CFS channels with no web holes, unstiffened web holes, and stiffened web holes may be
 374 approximated by

$$V_{cr} = \frac{k_v \pi^2 E (t_{eq})^3}{12(1 - \nu^2) d_1} \quad (11)$$

375

376 where t_{eq} is the equivalent thickness reference to the thickness of the web with no holes. The
 377 calculation of t_{eq} can be simplified as it depends on $\left(\frac{d_w}{d_1}\right)$ and (ϕ) . Therefore, best-fit
 378 relationships were derived for CFS channels with unstiffened and stiffened web holes. The t_{eq}
 379 may be estimated as follows.

- 380 • For CFS channels with no web holes:

$$t_{eq} = t \quad (12)$$

381 t_{eq} is equivalent to the thickness of the web (t) as there are no holes present in the web.

382

383 • For CFS channels with unstiffened web holes:

$$t_{eq} = \left[1 - \left(\frac{d_w}{d_1} \right)^{0.55} \right]^{0.22} t \quad (13)$$

384 t_{eq} depends on web hole ratio $\left(\frac{d_w}{d_1} \right)$ only for unstiffened web hole cases.

385 • For CFS channels with stiffened web holes:

$$t_{eq} = \left[1 - \left(\frac{d_w}{d_1} \right)^{0.55} \right]^{0.22} \left[1 + 0.73 \left(\frac{d_w}{d_1} \right) \phi^{0.23} \right] t \quad (14)$$

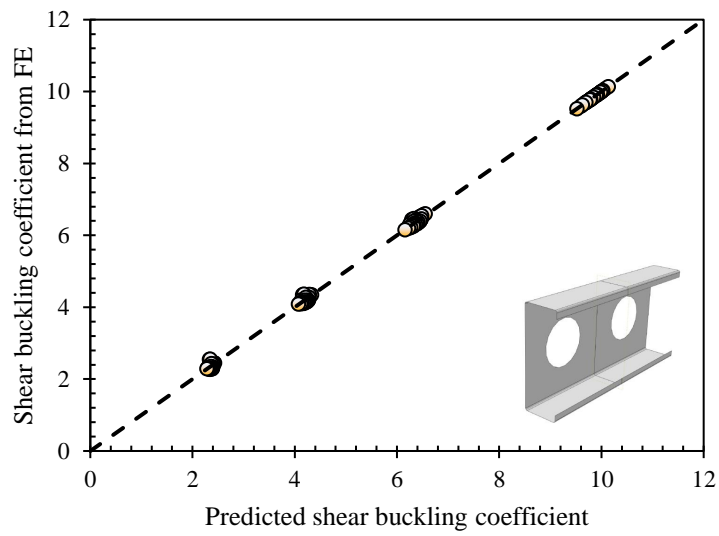
386 where $\left(\frac{d_w}{d_1} \right)$ is the web hole ratio as mentioned above and ϕ is the normalised factor that can
387 be determined from Eq. 10.

388 6. Assessment of new design proposals

389 In this section, the accuracy of the new design proposals to estimate the elastic shear
390 buckling strength of CFS channels with unstiffened and stiffened web holes is assessed against
391 the generated numerical data in Section 3.2.

392 Fig. 11 demonstrates the comparison of elastic shear buckling coefficients (calculated
393 from the proposed modified shear buckling coefficient method) with the shear buckling
394 coefficients back-calculated from FE results for unstiffened web holes cases. As shown in Fig
395 11, the calculated results using the proposed modified shear buckling coefficient method
396 displayed a closest agreement with the numerical results for unstiffened web holes cases. This
397 comparison resulted in a mean of 1.00 and a COV of 0.018. Further, a similar comparison was
398 made for stiffened web hole cases using the proposed modified shear buckling coefficient
399 method. The comparison for this case is shown in Fig. 12 and it can be observed that predicted
400 points follow a much tighter trend compared with FE results, resulting in a mean value of 1.00
401 and COV of 0.079. It is therefore confirmed that the new design proposal of the modified shear

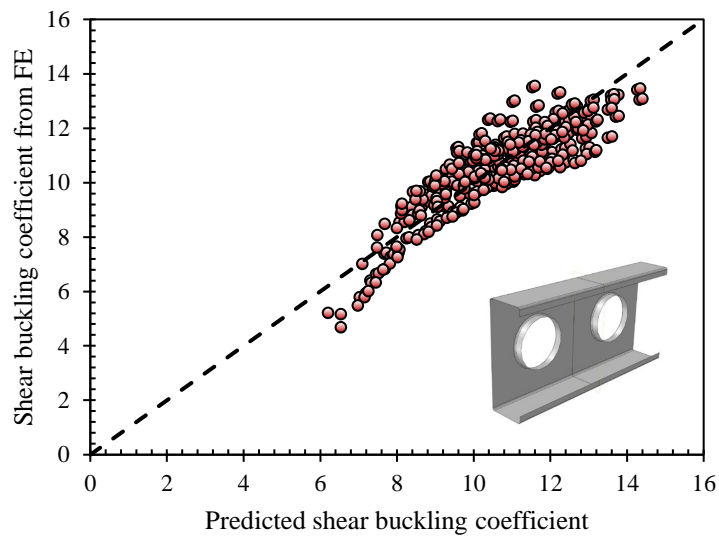
402 buckling coefficient method is capable of accurately estimating the elastic shear buckling
403 strength of CFS channels with unstiffened and stiffened web holes.



404

405 Fig. 11: Comparison of elastic shear buckling coefficients calculated using the proposed Eq. 9 with back-
406 calculated shear buckling coefficients from FE results for unstiffened web hole cases.

407



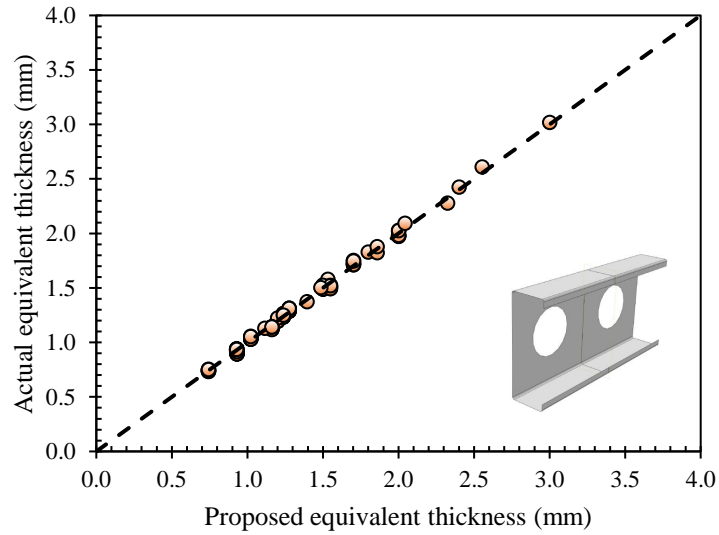
408

409 Fig. 12: Comparison of elastic shear buckling coefficients calculated using the proposed Eq. 10 with back-
410 calculated shear buckling coefficients from FE results for stiffened web hole cases.

411

412 The second design proposal was based on the equivalent thickness method. For the
413 unstiffened and stiffened web holes cases, the equivalent thicknesses determined using the
414 proposed equations were compared against the equivalent thicknesses back-calculated from FE
415 results. Fig. 13 depicts the comparison of elastic shear buckling strengths calculated using the
416 proposed equivalent thickness method with FE results for unstiffened web hole cases. The
417 comparison resulted in a mean and COV of 1.00 and 0.019, respectively, demonstrating a
418 higher level of accuracy. Similarly, the equivalent thicknesses determined from proposed
419 equations were compared against the equivalent thicknesses back-calculated using FE results
420 for stiffened web hole cases, illustrated in Fig. 14. The comparison shows a good agreement
421 between predicted and FE results with a mean of 1.00 and COV of 0.028. It is therefore
422 confirmed that the new design proposal of equivalent thickness method can be used to estimate
423 the elastic shear buckling strength of CFS channels with unstiffened and stiffened web holes
424 accurately.

425 The results and proposed equations in this paper can be used in conjunction with the
426 DSM-based shear design approach, as the DSM approach requires elastic shear buckling
427 strength to estimate the ultimate shear strength. Further, the results and proposed equations in
428 this paper will be a benchmark for studying the elastic shear buckling of CFS channels with
429 high aspect ratios where the influence of bending comes into account.



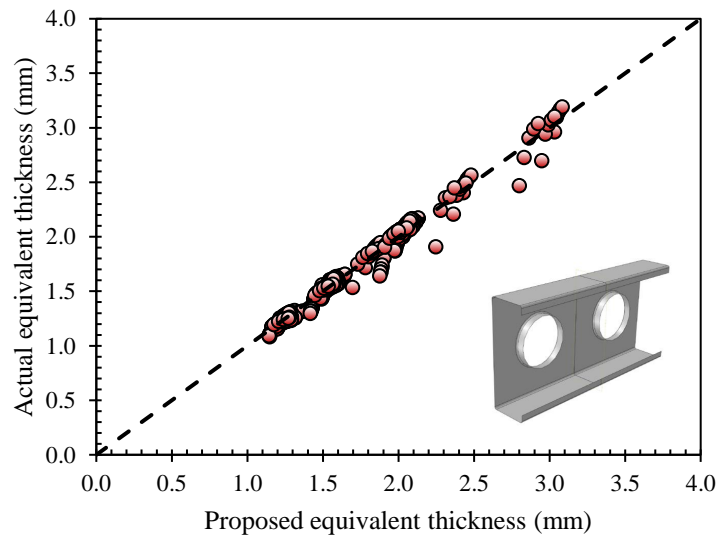
430

431

Fig. 13: Comparison of the equivalent thickness of the web calculated using the proposed Eq. 13 with actual required equivalent thickness back-calculated using FE results for unstiffened web hole cases.

432

433



434

435

Fig 14: Comparison of the equivalent thickness of the web calculated using the proposed Eq. 14 with actual required equivalent thickness back-calculated using FE results for stiffened web hole cases.

436

437 **7. Conclusions**

438

439

440

A numerical study into the elastic shear buckling response of cold-formed steel (CFS) channels with stiffened web holes has been conducted and presented in this paper. In total 551 finite element (FE) models were studied in the numerical programme: 29 CFS channels with

441 no holes, 87 with unstiffened circular web holes, and 435 edge stiffened circular web holes.
442 The validity of the developed FE models was ensured by comparing shear buckling strength
443 data with existing design proposals. A new unified design approach is proposed to estimate the
444 elastic shear buckling strength of CFS channels with no web holes, unstiffened web holes, and
445 stiffened web holes. Based on the results and analysis presented in this paper, the following
446 conclusions can be drawn:

447 (1) The average elastic shear buckling strength reductions due to the unstiffened web
448 holes with respect to CFS channels with no holes were 65%, 42%, and 24% for 0.3, 0.5, and
449 0.8 web hole ratios (diameter of the web hole / clear height of the web), respectively. The
450 numerical data of CFS channels with no holes showed a greater accuracy with Keerthan and
451 Mahendran [36]'s design proposal while Pham [36]'s design proposal may be appropriate for
452 CFS channels with unstiffened web holes as it also resulted in good agreement with numerical
453 data.

454 (2) Edge stiffeners improve the elastic shear buckling strength and are capable to regain
455 the elastic shear buckling strength reduction due to the web holes. However, it was found that
456 the degree of increment in the shear buckling strength is decreasing with the stiffener length.
457 This is because with increasing edge stiffener length, the buckling of edge stiffener can be more
458 easily observed.

459 (3) A new design is proposed using a unified shear buckling coefficient (k_v) to cover
460 all the different cases of no web holes, unstiffened web holes, and stiffened web holes.
461 Assessment of this design approach showed a greater accuracy with mean value of 1.00 and
462 COV of 0.018 for unstiffened web hole cases and mean value of 1.00 and COV of 0.079 for
463 stiffened web hole cases.

464 (4) As an alternative to the first design proposal, the effect of unstiffened web holes and
465 stiffened web holes on elastic shear buckling strength is captured using the equivalent thickness

466 method. Greater accuracy of this design proposal was observed as the assessment showed mean
467 value of 1.00 and COV of 0.019 for unstiffened web hole cases and mean value of 1.00 and
468 COV of 0.028 for stiffened web hole cases.

469 (5) A normalised factor (ϕ) has been introduced to reflect the influence of edge
470 stiffener and associated parameters on the elastic shear buckling strength. This factor is used
471 alongside with web hole ratio ($\frac{d_w}{d_1}$) to form the new design proposals.

472 (6) The proposed two design methods (modified shear buckling coefficient and
473 equivalent thickness method) are sufficiently straightforward for application in structural
474 engineering practice.

475 **Acknowledgements**

476 The technical support provided by Teesside University is appreciated. The first author
477 gratefully acknowledges the software facilities used at Northumbria University when he was
478 there.

479 **References**

- 480 [1] P. Keerthan, M. Mahendran, Experimental investigation and design of lipped channel beams in
481 shear, *Thin-Walled Structures* 86 (2015) 174-184.
482 [2] P. Keerthan, M. Mahendran, Improved shear design rules of cold-formed steel beams, *Engineering*
483 *Structures* 99 (2015) 603-615.
484 [3] P. Keerthan, M. Mahendran, New design rules for the shear strength of LiteSteel beams, *Journal of*
485 *Constructional Steel Research* 67(6) (2011) 1050-1063.
486 [4] P. Keerthan, M. Mahendran, Experimental studies on the shear behaviour and strength of LiteSteel
487 beams, *Engineering Structures* 32(10) (2010) 3235-3247.
488 [5] P. Keerthan, M. Mahendran, Numerical Modeling of LiteSteel Beams Subject to Shear, *Journal of*
489 *Structural Engineering* 137(12) (2011) 1428-1439.
490 [6] P. Keerthan, M. Mahendran, A. Narsey, Shear tests of hollow flange channel beams with real
491 support conditions, *Structures* 3 (2015) 109-119.
492 [7] C.H. Pham, G.J. Hancock, Direct Strength Design of Cold-Formed C-Sections for Shear and
493 Combined Actions, *Journal of Structural Engineering* 138(6) (2012) 759-768.
494 [8] C.H. Pham, G.J. Hancock, Numerical simulation of high strength cold-formed purlins in combined
495 bending and shear, *Journal of Constructional Steel Research* 66(10) (2010) 1205-1217.
496 [9] P. Gatheeshgar, K. Poologanathan, S. Gunalan, B. Nagaratnam, K.D. Tsavdaridis, J. Ye, Structural
497 behaviour of optimized cold-formed steel beams, *Steel Construction* 13(4) (2020) 294-304.

498 [10] P. Gatheeshgar, K. Poologanathan, S. Gunalan, I. Shyha, K.D. Tsavdaridis, M. Corradi, Optimal
499 design of cold-formed steel lipped channel beams: Combined bending, shear, and web crippling,
500 Structures 28 (2020) 825-836.

501 [11] EN1993-1-3, Eurocode 3: Design of steel structures - Part 1-3: General rules - Supplementary rules
502 for cold-formed members and sheeting, European Committee for Standardization (CEN), Brussels,
503 Belgium, 2006.

504 [12] AISI-S100, North American Specification for the Design of Cold-Formed Steel Structural Members,
505 American Iron and Steel Institute 2016.

506 [13] AS/NZS-4600, Australian/New Zealand Standard Cold-Formed Steel Structures, Sydney, Australia,
507 2018.

508 [14] S.H. Pham, C.H. Pham, C.A. Rogers, G.J. Hancock, Shear Strength Experiments and Design of Cold-
509 Formed Steel Channels with Web Holes, Journal of Structural Engineering 146(1) (2020).

510 [15] C.H. Pham, G.J. Hancock, Shear tests and design of cold-formed steel channels with central square
511 holes, Thin-Walled Structures 149 (2020).

512 [16] V.V. Degtyarev, N.V. Degtyareva, Finite element modeling of cold-formed steel channels with solid
513 and slotted webs in shear, Thin-Walled Structures 103 (2016) 183-198.

514 [17] N.V. Degtyareva, V.V. Degtyarev, Experimental investigation of cold-formed steel channels with
515 slotted webs in shear, Thin-Walled Structures 102 (2016) 30-42.

516 [18] R.A. LaBoube, W.W. Yu, J.E. Langan, M.Y. Shan, Cold-Formed Steel Webs with Openings: Summary
517 Report, Thin-Walled Structures 27 (1997) 79-84.

518 [19] D.K. Pham, C.H. Pham, G.J. Hancock, Parametric study for shear design of cold-formed channels
519 with elongated web openings, Journal of Constructional Steel Research 172 (2020).

520 [20] S.H. Pham, C.H. Pham, G.J. Hancock, Direct Strength Method of Design for Channel Sections in
521 Shear with Square and Circular Web Holes, Journal of Structural Engineering 143(6) (2017).

522 [21] D.K. Pham, C.H. Pham, S.H. Pham, G.J. Hancock, Experimental investigation of high strength cold-
523 formed channel sections in shear with rectangular and slotted web openings, Journal of Constructional
524 Steel Research 165 (2020).

525 [22] P. Keerthan, M. Mahendran, Improved shear design rules for lipped channel beams with web
526 openings, Journal of Constructional Steel Research 97 (2014) 127-142.

527 [23] M.F.M. Ishqy, S. Wanniarachchi, K. Poologanathan, S. Gunalan, P. Gatheeshgar, T.
528 Suntharalingam, S. Navaratnam, Shear behaviour of cold-formed stainless-steel beams with web
529 openings: Numerical studies, Structures 31 (2021) 127-144.

530 [24] P. Keerthan, M. Mahendran, Shear Behaviour and Strength of LiteSteel Beams with Web
531 Openings, Advances in Structural Engineering 15(2) (2012) 171-184.

532 [25] P. Keerthan, M. Mahendran, Experimental studies of the shear behaviour and strength of lipped
533 channel beams with web openings, Thin-Walled Structures 73 (2013) 131-144.

534 [26] P. Keerthan, M. Mahendran, New Design Rules for the Shear Strength of LiteSteel Beams with
535 Web Openings, Journal of Structural Engineering 139(5) (2013) 640-656.

536 [27] A.M. Yousefi, B. Samali, Y. Yu, Shear behaviour and design of cold-formed ferritic stainless steel
537 channels with circular web openings, Structures 33 (2021) 4162-4175.

538 [28] K.S. Wanniarachchi, M. Mahendran, P. Keerthan, Shear behaviour and design of Lipped Channel
539 Beams with non-circular web openings, Thin-Walled Structures 119 (2017) 83-102.

540 [29] K. Thirunavukkarasu, E. Kanthasamy, K. Poologanathan, K.D. Tsavdaridis, P. Gatheeshgar, S.
541 Hareindirasarma, A. McIntosh, Shear performance of SupaCee sections with openings: Numerical
542 studies, Journal of Constructional Steel Research 190 (2022).

543 [30] D.L. Chandramohan, E. Kanthasamy, P. Gatheeshgar, K. Poologanathan, M.F.M. Ishqy, T.
544 Suntharalingam, T. Kajaharan, Shear behaviour and design of doubly symmetric hollow flange beam
545 with web openings, Journal of Constructional Steel Research 185 (2021).

546 [31] P. Keerthan, M. Mahendran, Suitable stiffening systems for LiteSteel beams with web openings
547 subjected to shear, Journal of Constructional Steel Research 80 (2013) 412-428.

- 548 [32] M. Mahendran, P. Keerthan, Experimental studies of the shear behavior and strength of LiteSteel
549 beams with stiffened web openings, *Engineering Structures* 49 (2013) 840-854.
- 550 [33] B. Chen, K. Roy, Z. Fang, A. Uzzaman, C.H. Pham, G.M. Raftery, J.B.P. Lim, Shear Capacity of Cold-
551 Formed Steel Channels with Edge-Stiffened Web Holes, Unstiffened Web Holes, and Plain Webs,
552 *Journal of Structural Engineering* 148(2) (2022).
- 553 [34] E. Kanthasamy, K. Thirunavukkarasu, K. Poologanathan, P. Gatheeshgar, S. Todhunter, T.
554 Suntharalingam, M. Fareedh Muhammadh Ishqy, Shear behaviour of doubly symmetric rectangular
555 hollow flange beam with circular edge-stiffened openings, *Engineering Structures* 250 (2022).
- 556 [35] P. Keerthan, M. Mahendran, Elastic shear buckling characteristics of LiteSteel beams, *Journal of*
557 *Constructional Steel Research* 66(11) (2010) 1309-1319.
- 558 [36] P. Keerthan, M. Mahendran, Shear buckling characteristics of cold-formed steel channel beams,
559 *International Journal of Steel Structures* 13(3) (2013) 385-399.
- 560 [37] C.H. Pham, G.J. Hancock, Shear buckling of thin-walled channel sections, *Journal of Constructional*
561 *Steel Research* 65(3) (2009) 578-585.
- 562 [38] C.H. Pham, G.J. Hancock, Elastic buckling of cold-formed channel sections in shear, *Thin-Walled*
563 *Structures* 61 (2012) 22-26.
- 564 [39] C.H. Pham, Shear buckling of plates and thin-walled channel sections with holes, *Journal of*
565 *Constructional Steel Research* 128 (2017) 800-811.
- 566 [40] ABAQUS, Hibbitt, Karlsson & Sorensen, Inc., Paw-tucket, USA, 2017.
- 567 [41] S.P. Timoshenko, J.M. Gere, *Theory of Elastic Stability*, McGraw-Hill Book Inc, New York, 1961.
- 568 [42] S.C. Lee, J.S. Davidson, C.H. Yoo, Shear Buckling Coefficients of Plate Girder Web Panels,
569 *Computers & Structures* 59(5) (1996) 789-795.
- 570 [43] D.M.M.P. Dissanayake, K. Poologanathan, S. Gunalan, K.D. Tsavdaridis, K.S. Wanniarachchi, B.
571 Nagaratnam, Numerical investigation of cold-formed stainless steel lipped channels with longitudinal
572 stiffeners subjected to shear, *Thin-Walled Structures* 158 (2021).

573